Journal of Pediatric Neuroradiology 3 (2014) 63–73
DOI 10.3233/PNR-14088
IOS Press

Cerebral Blood Flow and DTI metrics changes in children with cerebral palsy following therapy

Krishan K. Jain[a,g], Vimal K. Paliwal[b], Abhinav Yadav[c], Bhaswati Roy[a,g], Puneet Goel[d], Saurabh Chaturvedi[a], Ankita Chaurasia[a], Ravindra K. Garg[e], Ram K.S. Rathore[f] and Rakesh K. Gupta[a,g,*]

[a]*Department of Radiodiagnosis, Sanjay Gandhi Postgraduate Institute of Medical Sciences, Lucknow, India*
[b]*Department of Neurology, Sanjay Gandhi Postgraduate Institute of Medical Sciences, Lucknow, India*
[c]*Department of Biological Sciences, Indian Institute of Science Education and Research, Kolkata, India*
[d]*Department of Anaesthesiology, Sanjay Gandhi Postgraduate Institute of Medical Sciences, Lucknow, India*
[e]*Department of Neurology, King George Medical University, Lucknow, India*
[f]*Department of Mathematics and Statistics, Indian Institute of Technology, Kanpur, India*
[g]*Departments of Radiology & Imaging, Fortis Memorial Research Institute, Gurgaon.*

Received 24 May 2013
Revised 16 December 2013
Accepted 29 December 2013

Abstract. It is known that patients with chronic hypoxia have regional changes in their cerebral blood flow (CBF). The purpose of this study was to observe the CBF and diffusion tensor imaging (DTI) metrics changes in children with cerebral palsy (CP) at baseline and after 6 months of treatment. Thirty-eight children with cerebral diplegia (mean age = 6.4 yr) and twenty-one age/sex matched controls (mean age = 7.5 yr) were evaluated by the Gross Motor Function Classification System (GMFCS) scoring of motor disability and modified Ashworth scoring of spasticity. All subjects underwent pseudo-continuous arterial spin labeling (PCASL) and DTI, in addition to conventional magnetic resonance imaging (MRI). Significant increase in CBF values was observed in several grey and white matter regions (including areas of abnormal T2 hyperintensity in the periventricular white matter) in CP children as compared to controls based upon voxel-wise analysis. Low fractional anisotropy (FA) and high apparent diffusion coefficient (ADC) values were observed in these areas of high CBF, using a region of interest (ROI) based analysis. On follow-up study, CBF values were found to be significantly higher in two grey matter areas and lower in three white matter regions in comparison to baseline; however no significant changes in DTI indices were observed in these regions. CBF values are high in CP children as compared to controls and show alteration following therapy even when the DTI metrics remain unchanged. Arterial spin labeling (ASL) may be added to the advanced imaging protocol for studying brain plasticity in such children in future.

Keywords: Cerebral palsy, cerebral blood flow, voxel wise analysis, diffusion tensor imaging, arterial spin labeling, brain

1. Introduction

CP is a non-progressive neurological disorder of infancy and childhood caused by abnormal development or damage to one or more parts of the brain. These result in abnormal muscle tone, motor weakness, dystonia, mental retardation and epilepsy [1]. Spastic quadriplegia and diplegia are the most common motor disabilities seen in children with CP [2]. The cerebral insult may occur antepartum, intrapartum, or after birth up to about age three. Vulnerability of an immature cerebral autoregulation to hypoxia or ischemia is considered as a prime factor responsible for the changes in the CBF and consequent cerebral damage in the most vulnerable brain regions during the acute phase of injury [3].

*Corresponding author: Dr. Rakesh K Gupta, MD, Director and Head, Department of Radiology and Imaging, Fortis Memorial Research Institute, Sector 44, Gurgaon, Haryana, 122002, India. Tel.: +91 971 798 8859; E-mail: rakeshree1@gmail.com.

The sequela of acute brain injury often appear as periventricular white matter changes on MRI [4]. Though conventional MRI can identify periventricular white matter injury, it does not give information about the extent of injury in specific white matter pathways [5]. Over the years, advanced imaging techniques such as DTI and diffusion tensor tractography have been performed in these children. Significant changes in DTI matrices in various brain regions are well documented in these children, including those with normal appearing brain on conventional MRI [5–7]. DTI measures have been shown to correlate with the clinical severity of motor disabilities in children with spastic diplegia and quadriplegia as assessed by the GMFCS scale [8]. FA values of motor and sensory tracts have been shown to be significantly lower in children with CP than in controls [9]. Significant increase of FA has been observed on six-month follow up after therapy with botulinum (BTX) combining physiotherapy as compared to baseline [10]. Another study has shown that DTI metrics of the corticospinal tract in quadriplegic and diplegic CP patients significantly corresponds to their typical clinical manifestation [11]. Hoon AH et al. [12] demonstrated that CP in preterm children reflects disruption of thalamocortical connections as well as descending corticospinal pathways. Considering abnormal cerebrovascular autoregulation and consequent ischemic changes in the developing brain as a result of hypoxic insult, study of CBF in these children using MR/CT perfusion imaging is of interest. Decreased or normal CBF has been reported in patients with CP using Xenon-133 inhalation single photon emission CT [13], however no study is available which quantifies CBF in these patients with MRI or CT. ASL uses magnetic labeling of protons in blood to provide an endogenous tracer of flow and is a noninvasive technique that quantifies CBF *in vivo*. A number of studies are available in the literature that describe the application of ASL in various disorders like stroke, hypoxic ischemic brain disorders, and brain tumors [14,15]. Combination of ASL and DTI has been used in showing relationship between cortical blood flow and sub-cortical white-matter integrity across the adult age span [16] and in posttraumatic stress disorder [17]. These two techniques have shown functional and structural changes in mild traumatic brain injury [18], Alzheimer's disease and fronto-temporal dementia [19].

We hypothesized that children with CP should have areas of altered vascular dynamics on ASL perfusion study in both normal and abnormal appearing brain regions on conventional MRI; additionally these areas should demonstrate altered DTI metrics. The aim of this study was to observe the CBF and DTI metrics changes and its possible clinical utility in children with CP following therapy.

2. Materials and methods

The study was approved by our Institutional ethics committee. Informed and written parental consent was obtained for all the children. The study was performed on 38 children with CP having spastic diplegia (male = 21, female = 17, mean age = 6.4 years, age range = 3–12yrs) and 21 age/sex matched controls (age range 3–11 years; male = 13, female = 8, mean age = 7.5 yrs). The effect of age was not statistically significant (T-test). Diagnosis of CP was made in all children on the basis of the following features: history of delayed crying after birth, delayed motor/mental milestones, spastic motor weakness of lower limbs, persistence of primitive reflexes and abnormal postural reflexes, and a non-progressive course of illness. Children with intelligence quotient (IQ) above 50 and below 69, considered to be suffering from mild mental retardation, were included in the study. Indian adaptation of the Revised Amsterdamse Kinder Intelligence (RAKIT) Test, also known as Indian Children Intelligence Test (ICIT), was performed on CP children by two of the co-authors (SC and AC) to evaluate IQ scores. None of the patients had a history of seizures. Severity of illness was assessed by using the GMFCS scale and spasticity was scored as per the modified Ashworth scale. The GMFCS scale is a five-level classification system for children with CP scaled as per increasing severity of motor difficulty assessed by self-initiated movement by the children with emphasis on sitting and walking. GMFCS and IQ scores were evaluated prior to enrollment of the children in the study. Children with CP received BTX A toxin injection (Dysport, Ipsen, United Kingdom) along with physiotherapy. The dose was 100–500 units/muscle depending on muscle bulk; the total dose did not exceed 30 units/kg body weight.

Conventional MRI, DTI and 3D PCASL were performed in all 38 children with CP and compared with data acquired from twenty-one age and sex matched controls. The MRI data of two CP children were excluded from the study due to motion artifact. The MRI protocol was repeated after 6 months of therapy (BTX A toxin injection and physiotherapy) in 10 children to look for any changes on imaging.

2.1. Sedation

MRI of all subjects was performed under sedation, which was performed by an experienced cardiac anesthesiologist. Prior to MRI, subjects were prepared by fasting: no solid food for at least 6 h and no fluids for 3 h. Subjects were sedated with intramuscular injection of ketamine (5 mg/kg) and glycopyrrolate (10 microgram/kg). After sedation, an intravenous cannula was secured in the ante-cubital vein for additional intravenous doses of ketamine (1 mg/kg) and midazolam (0.05 mg/kg), if required. Ketamine was used as it is not known to alter CBF following its administration [20]. Subjects were placed in the supine position in the MRI scanner and their oxygen saturation, respiration, blood pressure and cardiac rhythm were continuously monitored. After completion of MRI, subjects were moved to an adjoining recovery room and monitored until fully awake.

2.2. MRI imaging

Conventional MRI, DTI and 3D PCASL were performed using an eight channel (phased array) head coil on a 3T MR scanner (Signa Hdxt, General Electric, Milwaukee, USA). DTI data was acquired using a dual spin-echo single-short echo-planar sequence with 30 uniformly distributed directions and ramp sampling on. The acquisition parameters were: repetition time (TR) = 10 sec / echo time (TE) = 100 ms / number of slices = 46 / slice thickness = 3 mm / inter-slice gap = 0 / field of view (FOV) = 240 mm / image matrix = 256 × 256 / number of excitation (NEX) = 1 / diffusion weighting b-factor = 1000s mm^{-2} in addition to the reference measurement with b = 0 s mm^{-2} [21]. DTI data was processed by using JAVA based in-house developed DTI-software to obtain eigenvalues (λ_1, λ_2 and λ_3) and three orthonormal eigenvectors (e1, e2, e3) as described elsewhere [21,22]. These tensor field data were then used to compute the DTI metrics such as aADC [Eq. (1)] and fractional anisotropy [Eq. (2)] for each voxel [21,22].

$$ADC = \frac{\lambda_1 + \lambda_2 + \lambda_3}{3} \quad \text{(Eq.1)}$$

$$FA(\lambda_1,\lambda_2,\lambda_3) = \frac{1}{\sqrt{2}}\sqrt{\frac{(\lambda_1-\lambda_2)^2+(\lambda_2-\lambda_3)^2+(\lambda_1-\lambda_3)^2}{\lambda_1{}^2+\lambda_2{}^2+\lambda_3{}^2}} \quad \text{(Eq.2)}$$

The 3D PCASL was performed using 3D FSE spiral acquisition with eight in-plane spiral interleaves using the following parameters: NEX = 3 / no. of slices = 46 / FOV = 240 mm / slice thickness = 3 mm / band width = 62.5 Hz / post label delay (PLD) = 1025 ms / duration of tagging = 1450 ms / TR = 4511 ms / TE = 10.44 ms / acquisition matrix = 512 × 8 / reconstructed matrix = 128 × 128 with spiral acquisition along with 3D proton density (PD) weighted FSE. The parameters taken were the best considering scan time as a constraint. The equation of the model used for quantification of perfusion is:

$$CBF = 600*\lambda \frac{\left(1-\exp\left(-\frac{ST(s)}{T_{1t}(s)}\right)\right)\exp\left(\frac{PLD(s)}{T_{1b}(s)}\right)}{2T_{1b}(s)\left(1-\exp\left(-\frac{LT(s)}{T_{1b}(s)}\right)\right)\varepsilon * NEX_{PW}} \left(\frac{PW}{SF_{pw}PD}\right)$$

where T_{1b} represents T1 of blood and for 3T T_{1b} is assumed as 1.6s, ST is saturation time and set as 2s, PLD represents post labeling delay, LT is the labeling duration, NEX_{PW} is the number of excitation for perfusion weighted images, SF_{PW} represents the scaling factor of perfusion weighted sequence. The partition coefficient λ for whole brain is considered as 0.9 and the efficiency ε is a combination of both inversion (0.8) and background suppression efficiency (0.75) which results in overall efficiency of 0.6. The partial saturation of the reference image (PD) is corrected by using a T_{1t} of 1.2s (typical of gray matter). The CBF maps were generated in the scanner itself with background suppression [23].

2.3. Voxel-wise analysis

CBF maps were generated from ASL images using the scanner's software. The maps were spatially preprocessed using SPM8 (Statistical Parametric Mapping) [24,25]. The CBF maps were co-registered to the corresponding T1-weighted images and spatially normalized to a 2 × 2 × 2-mm^3 ''T1-template'' (Montreal Neurologic Institute) permitting voxel-wise analysis of the CBF maps in a common stereotactic space, and smoothed in space with a three-dimensional, 8-mm full width- at-half-maximum, Gaussian kernel [26,27].

2.4. ROI based analysis

The DTI metrics and CBF maps were co-registered using mutual information based registration technique

prior to voxel-wise registration [28,29]. ROIs were placed for obtaining ADC, FA, and CBF values simultaneously in various white matter and grey matter regions blinded to the results of voxel-wise analysis. Mean values of these parameters were also recorded in abnormal T2 hyperintense periventricular white matter in patients and were compared with controls.

2.5. Statistical analysis

Voxel-wise comparison was performed using the general linear model to look for changes in CBF among the patient group compared to the control group. The threshold for minimum number of voxels to be present in a cluster was set to 10 and a statistical significance of $p = 0.001$, after correcting for FWE (family-wise error correction), was considered. This removes the minor clusters with small number voxels which can crop up due to random effect. Student's Independent T test was performed for comparing ROI based DTI derived metrics and ROI based CBF values between controls and patients based on the regions obtained from voxel-wise analysis. Student's paired T test was performed to look for changes in baseline and after six months of therapy, DTI metrics and CBF values in the ROIs obtained from the voxel-wise analysis. P values of ≤ 0.05 were considered to be significant. All statistical analyses for ROI based values were performed using SPSS (version 16.0, SPSS Inc, Chicago, USA) statistical software.

3. Results

On the basis of GMFCS, all the patients were classified as grade II CP and had scores in the range of 50 to 60. Significant increases in GMFCS scores were observed on follow-up as compared to baseline following therapy in 10 children. On conventional MRI, abnormal imaging findings such as T1 hypo / isointense and T2/FLAIR hyperintense regions involving the periventricular white matter were seen in the 28 CP children, and in the remaining eight CP children such abnormalities were not found.

Global grey matter and white matter perfusion in children with CP was significantly higher than in controls. In grey matter and white matter, global CBF observed in patients was 62.26 ± 18.8 and 41.86 ± 12.32 ml/100 gm/min, respectively, and in controls was 46.61 ± 15.3 and 24.2 ± 8.5 ml/100 gm/min respectively. There was a significant change in global grey matter and white matter perfusion in children with CP at baseline than at follow-up: global CBF in grey matter and white matter at follow-up are 81.46 ± 20.4 and 41.25 ± 13.39 ml/100 gm/min respectively.

Significant differences in CBF, using ASL, were seen in seven grey-matter areas: right temporal, left parietal, right parietal, paracentral lobule, left frontal, right frontal and right precentral gyrus and in eight white matter regions: right temporal, left temporal, right parietal, left parietal, right frontal, left frontal, right occipital and left occipital showed significant increases in CBF values in children with CP as compared to controls. (Figs. 1 & 2 and Table 1).

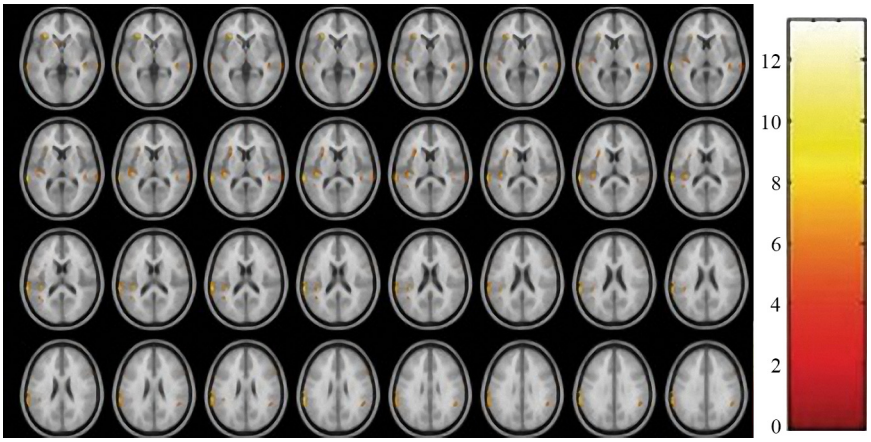

Fig. 1. Colored regions show areas with significant increase ($p < 0.001$, family-wise error corrected, with $k > 10$ voxels) in cerebral blood flow values on various grey matter regions in children with cerebral palsy as compared to controls overlaid on MNI template in axial plane. The right side of each section represents the right side of the brain. Color bar denotes T-values.

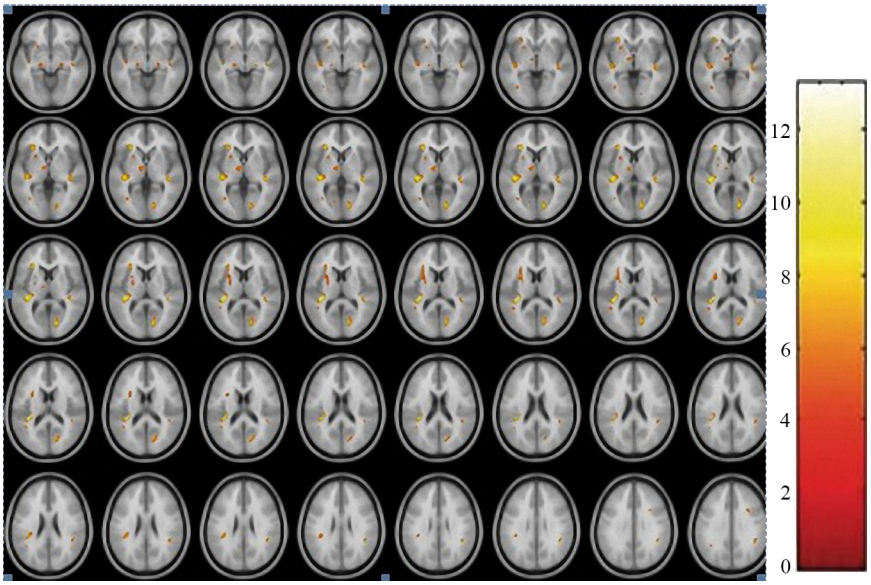

Fig. 2. Colored regions show areas with significant increase ($p<0.001$, family-wise error corrected, with $k>10$ voxels) in cerebral blood flow values on various white matter regions in children with cerebral palsy as compared to controls overlaid on MNI template in axial plane. The right side of each section represents the right side of the brain. Color bar denotes T-values.

Table 1
Grey and white matter regions with significant changes in cerebral blood flow values based upon voxel-wise analysis in children of cerebral palsy as compared to controls

Regions	MNI coordinates			Z score	PFWE-Corr	Changes
	X	Y	Z			
Temporal GM Rt	36	−7.5	10.5	7.087	0.0053	↑
Parietal GM Lt	−60	−12	22.5	6.518	0.0003	↑
Parietal GM Rt	28.5	−49.5	55.5	6.724	0.0051	↑
Paracentral Lobule	3	−45	64.5	6.926	0.0008	↑
Frontal GM Lt	−48	−1.5	30	7.047	0.0001	↑
Frontal GM Rt	49.5	3	25.5	6.507	0.0015	↑
Precentral Gyrus Rt	36	−9	52.5	6.66	0.0046	↑
Temporal WM Rt	40.5	−30	3	> 10	5.51E-07	↑
Temporal WM Lt	−36	−33	15	> 10	1.24E-12	↑
Parietal WM Rt	33	−57	39	5.570	0.0080	↑
Parietal WM Lt	−36	−33	24	7.824	1.24E-12	↑
Frontal WM Rt	31.5	24	7.5	5.648	0.0009	↑
Frontal WM Lt	−30	27	3	> 10	3.57E-10	↑
Occipital WM Rt	15	−78	6	> 10	2.57E-06	↑
Occipital WM Lt	−37.5	−51	37.5	> 10	1.24E-12	↑

↑: Increased In patient, Rt: Right, Lt: Left, WM: white matter, GM: grey matter, FWE-Corr: family-wise error correction

Areas of significant changes in CBF values on follow-up in comparison to baseline: increase in right frontal and left parietal grey matter, and significant decreases in CBF in three white matter areas: right parietal, left temporal and right temporal cortex. (Figs. 3 & 4 and Table 2).

Areas with significant changes in DTI indices (ADC & FA values) in regions with high CBF as determined by voxel-wise analysis: On post processed data of DTI, we found significant changes in either of ADC or FA values in two grey matter and eight white matter regions, which also showed high CBF on voxel wise analysis in children with CP in comparison to controls (Table 3).

DTI indices among regions with significant changes in CBF on follow up in comparison to baseline: We did

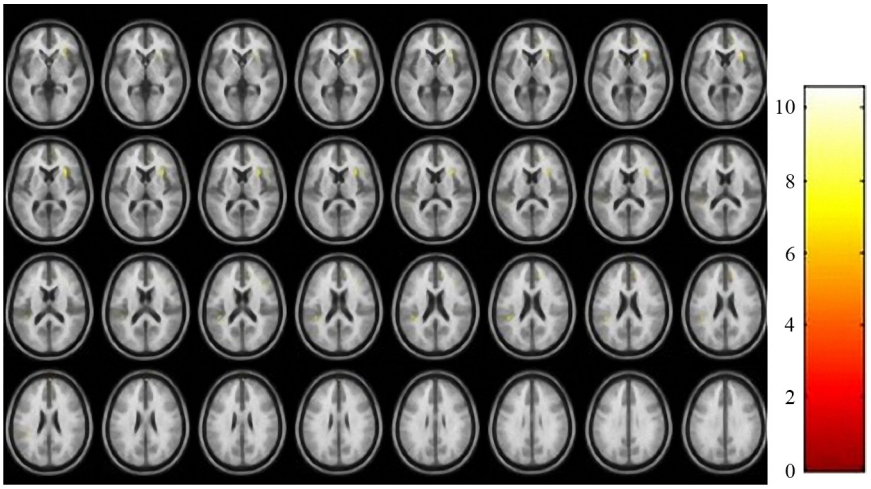

Fig. 3. Colored regions show areas with significant increase ($p<0.001$, family-wise error corrected, with $k>10$ voxels) in cerebral blood flow values in various grey matter regions in children with cerebral palsy on follow up in comparison to baseline study overlaid on MNI template in axial plane. The right side of each section represents the right side of the brain. Color bar denotes T-values.

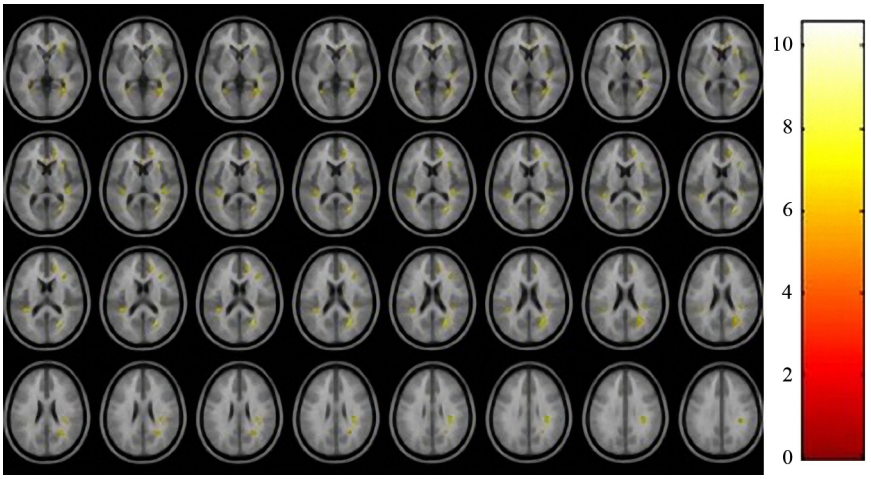

Fig. 4. Colored regions show areas with significant decrease ($p<0.001$, family-wise error corrected, with $k>10$ voxels) in cerebral blood flow values on various white matter regions in children with cerebral palsy on follow up in comparison to baseline study overlaid on MNI template in axial plane. The right side of each section represents the right side of the brain. Color bar denotes T-values.

Table 2
Grey and white matter regions with significant changes in cerebral blood flow values based upon voxel-wise analysis in children of cerebral palsy on follow up in comparison to baseline

Regions	MNI coordinates			Z score	PFWE-Corr	Changes
	X	Y	Z			
Frontal GM Rt	30	19.5	10.5	6.336	3.98E-05	↑
Parietal GM Lt	−42	−39	21	5.311	0.0026	↑
Parietal WM Rt	34.6029	−29.6439	28.1147	6.404	0	↓
Temporal WM Lt	−37.5	−33	9	5.530	4.33E-07	↓
Temporal WM Rt	34.5	−37.5	−3	6.230	0	↓

↑: Increased, ↓: Decreased, Rt: Right, Lt: Left, WM: white matter, GM: grey matter, FWE-Corr: family-wise error correction

Table 3
Grey and white matter regions with high cerebral blood flow (CBF) in children of cerebral palsy showing significant changes in either of apparent diffusion coefficient (ADC) and fractional anisotropy (FA) values with comparison to controls

Regions	Subject	CBF (ml/100 gm/min)	ADC ($\times 10^{-3}$ mm^2/s)	FA
Temporal GM Rt	Patient	69.589*	1.061	0.095*
	Control	54.117	1.004	0.130
Parietal GM Lt	Patient	72.592*	1.015	0.078*
	Control	60.270	0.984	0.101
Temporal WM Rt	Patient	73.547*	0.809	0.322*
	Control	62.423	0.782	0.384
Temporal WM Lt	Patient	65.932*	0.824*	0.300*
	Control	46.337	0.785	0.365
Parietal WM Rt	Patient	74.529*	0.826*	0.304*
	Control	57.124	0.791	0.351
Parietal WM Lt	Patient	62.534*	0.828*	0.302*
	Control	40.261	0.790	0.384
Frontal WM Rt	Patient	39.034*	0.907*	0.372
	Control	19.181	0.820	0.400
Frontal WM Lt	Patient	31.055*	0.879*	0.337
	Control	16.956	0.817	0.335
Occipital WM Rt	Patient	37.773*	0.892	0.381*
	Control	21.782	0.772	0.484
Occipital WM Lt	Patient	47.710*	0.921	0.391*
	Control	22.726	0.817	0.569

Rt: Right, Lt: Left, WM: white matter, GM: grey matter.
*Indicates significant changes.

Table 4
Apparent diffusion coefficient (ADC) and fractional anisotropy (FA) values among regions with significant changes in cerebral blood flow (CBF) observed in white and grey matter regions in children of cerebral palsy on follow up in comparison to baseline

Regions		CBF (ml/100 gm/min)	ADC ($\times 10^{-3}$ mm^2/s)	FA
Frontal GM Rt	Follow-up	63.865*	0.913	0.049
	Baseline	82.118	0.946	0.053
Parietal GM Lt	Follow-up	63.680*	1.053	0.076
	Baseline	81.839	0.936	0.089
Parietal WM Rt	Follow-up	61.840*	0.888	0.323
	Baseline	43.576	0.887	0.335
Temporal WM Lt	Follow-up	68.702*	0.844	0.255
	Baseline	59.002	0.837	0.253
Temporal WM Rt	Follow-up	69.809*	0.847	0.309
	Baseline	56.222	0.856	0.305

Rt: Right, Lt: Left, WM: white matter, GM: grey matter.
*Indicates significant changes.

not find any significant changes in DTI indices among regions which showed significant changes in CBF on follow-up in comparison to baseline (Table 4).

CBF and DTI values in periventricular white matter with abnormal T2 hyperintensity: Significant increase in the mean CBF was observed in periventricular white matter with abnormal signal intensity changes on T2 weighted images (Fig. 5a). We also found significant increases in mean ADC values with decrease in mean FA in corresponding areas using ROI based analysis (Fig. 5b).

4. Discussion

In this study significantly raised CBF values were found in CP children in normal appearing multiple grey and white matter regions as well as in areas of

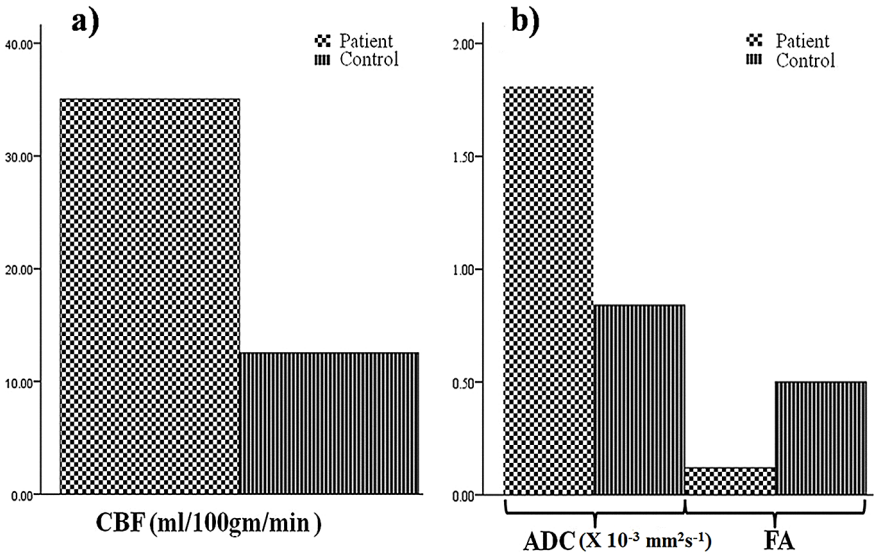

Fig. 5. Relative changes in mean cerebral blood flow (a) and mean apparent diffusion coefficient, mean fractional anisotropy (b) values in abnormal T2 hyperintense periventricular white matter regions in children with cerebral palsy as compared to controls.

abnormal T2 hyperintensity in periventricular white matter, compared to controls based on voxel-wise analysis. We also observed low FA and high ADC values in these areas of high CBF. In addition, we also observed increased CBF in some of the grey matter regions and decreases in CBF in some of the white matter regions following therapy in 10 of the CP children. Decreased FA in the various white matter regions has been established as a marker of disorganized or loss of structural barriers to molecular diffusion of water denoting the damaged brain regions secondary to hypoxia in children with CP [6–8].

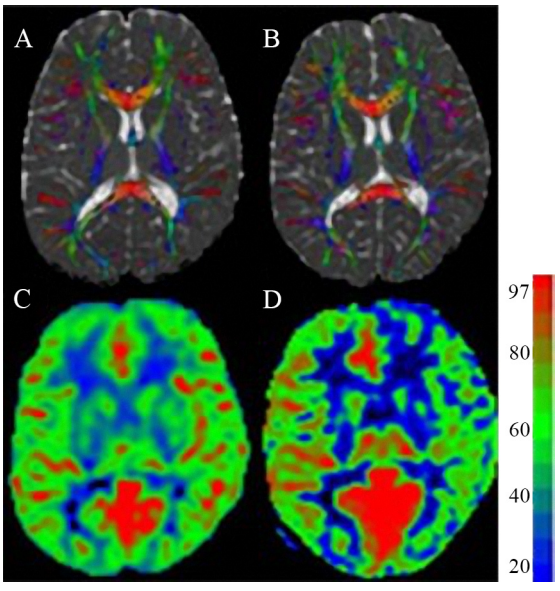

Fig. 6. Color-coded fractional anisotropy map overlaid on ADC image and cerebral blood flow map of (a), (c) pre therapy (b), (d) after 6 months of therapy (BTX A toxin injection and physiotherapy) of a patient with cerebral palsy. Color bar denotes CBF values in ml/100 gm/min.

Quantitative estimation of CBF using ASL perfusion MRI has been used for more than two decades in various disorders: stroke, hypoxic ischemic brain disorders, and brain tumors [14,15,22]. The cause of increased CBF in hypoxic-ischemic encephalopathy like CP is not well documented. One of the postulated mechanisms is the loss of autoregulation of cerebral arterioles. Globally increased CBF has been reported using ASL technique in patients successfully resuscitated from cardio-respiratory arrest resulting in acute hypoxic brain injury [30,31]. Loss of cerebrovascular adaptability can be related to the development of intraventricular hemorrhage and periventricular leukomalacia in neonates [32,33]. Impairment of cerebrovascular autoregulation has been demonstrated using an oxygen inhalation test in chronically hypoxic human and animal fetuses [34–36]. In chronic and severe hypoxia, fetal deterioration has been characterized by the disappearance of the physiological cerebral vascular variability (vasoconstriction and vasodilatation) followed by an increase in cerebral vascular resistance

(CVR) [37]. Autoregulation of CBF maintains the relationship CBF = cerebral perfusion pressure (CPP) / CVR. Possibly as a sequel to hypoxia, the cerebral arterioles lose their capacity to constrict and dilate leading to constant CVR. In such situations, CBF is directly proportional to CPP which is defined as mean arterial pressure minus intracranial pressure and thus, CBF becomes directly proportional to the mean arterial pressure [31,38–40]. There is little human data regarding the effect of global anoxia on autoregulation; however in animal models it has been reported that loss of cerebral vascular resistance in the postanoxic state results in uncontrolled hyperperfusion [41–49]. In a recent study, Strouse et al. [50] found an inverse correlation between CBF, measured by continuous arterial spin-labeling, and intelligence quotient (IQ) in children with sickle cell anemia. They postulated that increased CBF could be both a response to -and a risk factor for -cerebral hypoxia. In another study, done more than 20 years ago, Prohovnik et al. [51] demonstrated increased CBF in patients with sickle cell disease using 123-Xenon inhalation. They proposed that increased CBF resulted from adaptive vasodilatation. By the age of late infancy and early childhood, the time CBF estimation was done in our study, elevated CBF due to loss of cerebral autoregulation could be a compensatory response to reduced cerebral blood flow and resultant hypoxic damage that occurred during intra/peripartum period. This may be nature's attempt to revascularization of hypoxic brain regions in order to recover some functionality.

A recent study has shown increased CBF on SPECT in children with severe traumatic brain injury (TBI) who were imaged 3 years following trauma; they explained it on the basis of delayed brain maturation [52]. Hyperperfusion observed in CP children in the current study could also be related to delay in brain maturation or to a lag in the development of their brain function. Another plausible explanation for increased CBF in our study could be related to alteration in the γ-aminobutyric acid (GABA) receptor activity. In an animal study, Chi et al. [53] showed that blockade of $GABA_A$ receptors led to a significant increase in rCBF and blood brain barrier (BBB) permeability in the focal ischemic area.

In the current study, we also observed significant decreases in CBF in few of the white matter regions and significant increases in CBF in few of the grey matter regions on the follow-up study compared to baseline. However, we did not find any significant alteration in ADC and FA values in corresponding regions. Hyperperfusion of the grey matter regions is likely related to cortical plasticity or reorganization. In other words, increased perfusion indicates compensation as behavioral functions are displaced to brain regions other than the injured brain regions. Increase in resting state rCBF in contralesional premotor and prefrontal cortex suggests that reorganization associated with recovery of motor skills in stroke patients is associated with increased synaptic activity attributable to long term neuronal plasticity changes [54]. Metabolic changes were observed in cerebral cortex in children with strabismus along with increased perfusion on follow-up study after BTX injection [55]. This could be another explanation for hyperperfusion following treatment related to the drug therapy (BTX A toxin injection). Hypoperfusion of the white matter regions on follow-up could be related to decrease in CBF with brain maturation [56].

This study quantified changes in CBF only in grade II CP and has not been extended to all grades of the disease; this may be considered a limitation of this study. Another limitation of the study could be due to the partial volume affects in voxel-wise analysis (between grey and white matter) on low resolution perfusion maps which can confound real differences in CBF between groups. Also, it is uncertain if ASL techniques can accurately measure white matter perfusion on a voxel-to-voxel basis due to slow flow. However, the findings of voxel-wise analysis have been verified with ROI based analysis. Further experiments in future could be planned which may differentiate the specificity of ASL for measuring response to therapy and its usefulness as a biomarker for plasticity. Though ketamine was given to both patients and controls for sedation, its effect on CBF cannot be underestimated and can be considered as a potential confounding variable in the CBF estimates. Another limitation was the lack of optimization of post labeling delay time in ASL for these children.

We conclude that CBF values are increased in children with CP in various grey and white matter regions which have reduced FA and increased ADC values. Alteration in the CBF values in some of the grey and white matter regions following treatment with no significant changes in the DTI metrics suggest that CBF change may be an earlier predictor of plasticity than DTI indices and may be used in addition to the DTI metrics to study brain plasticity.

Acknowledgment

Grant support: This study is supported by Department of Science & Technology (Grant No. SR/SO/

HS/125/2007), New Delhi, India. Saurabh Chaturvedi and Ankita Chaurasia acknowledges financial support from DST, New Delhi, India.

References

[1] Mutch L, Alberman E, Hagberg B, Kodama K, Perat MV. Cerebral palsy epidemiology: where are we now and where are we going? Dev Med Child Neurol 1992;34(6):547–51.
[2] Gladstone M. A review of the incidence and prevalence, types and aetiology of childhood cerebral palsy in resource-poor settings. Ann Trop Paediatr 2010;30(3):181–96.
[3] Rezaie P, Dean A. Periventricular leukomalacia, inflammation and white matter lesions within the developing nervous system. Neuropathology 2002;22(3):106–32.
[4] Lee JD, Park HJ, Park ES, Oh MK, Park B, Rha DW, et al. Motor pathway injury in patients with periventricular leucomalacia and spastic diplegia. Brain 2011;134(Pt 4): 1199–210.
[5] Hoon AH Jr, Stashinko EE, Nagae LM, Lin DD, Keller J, Bastian A, et al. Sensory and motor deficits in children with cerebral palsy born preterm correlate with diffusion tensor imaging abnormalities in thalamocortical pathways. Dev Med Child Neurol 2009;51(9):697–704.
[6] Berman JI, Mukherjee P, Partridge SC, Miller SP, Ferriero DM, Barkovich AJ, et al. Quantitative diffusion tensor MRI fiber tractography of sensorimotor white matter development in premature infants. Neuroimage 2005;27(4):862–71.
[7] Hoon AH Jr, Lawrie WT Jr, Melhem ER, Reinhardt EM, Van Zijl PC, Solaiyappan M, et al. Diffusion tensor imaging of periventricular leukomalacia shows affected sensory cortex white matter pathways. Neurology 2002;59(5):752–6.
[8] Trivedi R, Agarwal S, Shah V, Goyel P, Paliwal VK, Rathore RK, et al. Correlation of quantitative sensorimotor tractography with clinical grade of cerebral palsy. Neuroradiology 2010;52(8):759–65.
[9] Yoshida S, Hayakawa K, Yamamoto A, Okano S, Kanda T, Yamori Y, et al. Quantitative diffusion tensor tractography of the motor and sensory tract in children with cerebral palsy. Dev Med Child Neurol 2010;52(10):935–40.
[10] Chaturvedi SK, Rai Y, Chourasia A, Goel P, Paliwal VK, Garg RK, et al. Comparative assessment of therapeutic response to physiotherapy with or without botulinum toxin injection using diffusion tensor tractography and clinical scores in term diplegic cerebral palsy children. Brain Dev 2013;35(7): 647–53.
[11] Chang MC, Jang SH, Yoe SS, Lee E, Kim S, Lee DG, et al. Diffusion tensor imaging demonstrated radiologic differences between diplegic and quadriplegic cerebral palsy. Neurosci Lett 2012;512(1):53–8.
[12] Hoon AH Jr, Stashinko EE, Nagae LM, Lin DD, Keller J, Bastian A, et al. Sensory and motor deficits in children with cerebral palsy born preterm correlate with diffusion tensor imaging abnormalities in thalamocortical pathways. Dev Med Child Neurol 2009;51(9):697–704.
[13] Taudorf K, Vorstrup S. Cerebral blood flow abnormalities in cerebral palsied children with a normal CT scan. Neuropediatrics 1989;20(1):33–40.
[14] Melzer TR, Watts R, MacAskill MR, Pearson JF, Rüeger S, Pitcher TL, et al. Arterial spin labelling reveals an abnormal cerebral perfusion pattern in Parkinson's disease. Brain 2011;134(Pt 3):845–55.
[15] Martirosian P, Boss A, Schraml C, Schwenzer NF, Graf H, Claussen CD, et al. Magnetic resonance perfusion imaging without contrast media. Eur J Nucl Med Mol Imaging 2010; 37 Suppl 1:S52–64.
[16] Chen JJ, Rosas HD, Salat DH. The relationship between cortical blood flow and sub-cortical white-matter health across the adult age span. Plos One 2013;8(2):e56733.
[17] Schuff N, Zhang Y, Zhan W, Lenoci M, Ching C, Boreta L, et al. Patterns of altered cortical perfusion and diminished subcortical integrity in posttraumatic stress disorder: an MRI study. Neuroimage 2011;54 Suppl 1:S62–8.
[18] Grossman EJ, Jensen JH, Babb JS, Chen Q, Tabesh A, Fieremans E, et al. Cognitive impairment in mild traumatic brain injury: a longitudinal diffusional kurtosis and perfusion imaging study. AJNR Am J Neuroradiol 2013;34(5):951–7, S1–3.
[19] Zhang Y, Schuff N, Ching C, Tosun D, Zhan W, Nezamzadeh M, et al. Joint assessment of structural, perfusion, and diffusion MRI in Alzheimer's disease and frontotemporal dementia. Int J Alzheimers Dis 2011;2011:546871.
[20] Mayberg TS, Lam AM, Matta BF, Domino KB, Winn HR. Ketamine does not increase cerebral blood flow velocity or intracranial pressure during isoflurane/nitrous oxide anesthesia in patients undergoing craniotomy. Anesth Analg 1995;81(1): 84–9.
[21] Awasthi R, Verma SK, Haris M, Singh A, Behari S, Jaiswal AK, et al. Comparative evaluation of dynamic contrast-enhanced perfusion with diffusion tensor imaging metrics in assessment of corticospinal tract infiltration in malignant glioma. J Comput Assist Tomogr 2010;34(1):82–8.
[22] Purwar A, Rathore DK, Rathore RKS, Gupta RK. A DT-MRI analysis tool. Book of abstracts: Twenty third Annual Meeting of European Society for Magnetic Resonance in Medicine and Biology, Warsaw, Poland: ESMRMB; 2006. p. 644.
[23] Roy B, Awasthi R, Bindal A, Sahoo P, Kumar R, Behari S, et al. Comparative evaluation of 3-dimensional pseudocontinuous arterial spin labeling with dynamic contrast-enhanced perfusion magnetic resonance imaging in grading of human glioma. J Comput Assist Tomogr 2013;37(3):321–6.
[24] Ashburner J, Friston KJ. Voxel-based morphometry- the methods. Neuroimage 2000;11(6 Pt 1):805–21.
[25] Ashburner J. SPM: a history. Neuroimage 2012;62(2):791–800.
[26] Rao H, Wang J, Giannetta J, Korczykowski M, Shera D, Avants BB, et al. Altered resting cerebral blood flow in adolescents with in utero cocaine exposure revealed by perfusion functional MRI. Pediatrics 2007;120(5):e1245–54.
[27] Dashjamts T, Yoshiura T, Hiwatashi A, Yamashita K, Monji A, Ohyagi Y, et al. Simultaneous arterial spin labeling cerebral blood flow and morphological assessments for detection of Alzheimer's disease. Acad Radiol 2011;18(12):1492–9.
[28] Awasthi R, Verma SK, Haris M, Singh A, Behari S, Jaiswal AK, et al. Comparative evaluation of dynamic contrast-enhanced perfusion with diffusion tensor imaging metrics in assessment of corticospinal tract infiltration in malignant glioma. J Comput Assist Tomogr 2010;34(1):82–8.
[29] Verma SK, Rathore RKS, Gupta RK, Singh A, Purwar A, Bayu G, et al. Fusion of DT-MRI and DCE-MRI using binary search maximization of mutual information based registration. In: Proceedings of the 25th Annual Meeting of ESMRMB, Valencia/ES, 2008 (abstract 701).
[30] Pollock JM, Tan H, Kraft RA, Whitlow CT, Burdette JH, Maldjian JA. Arterial spin-labeled MR perfusion imaging: clinical applications. Magn Reson Imaging Clin N Am 2009;17(2): 315–38.

[31] Pollock JM, Whitlow CT, Deibler AR, Tan H, Burdette JH, Kraft RA, et al. Anoxic injury-associated cerebral hyperperfusion identified with arterial spin-labeled MR imaging. AJNR Am J Neuroradiol 2008;29(7):1302–7.
[32] Volpe JJ. Brain injury in the premature infant: Overview of clinical aspects, neuropathology, and pathogenesis. Semin Pediatr Neurol 1998;5(3):135–51.
[33] Funato M, Tamai H, Noma K, Kurita T, Kajimoto Y, Yoshioka Y, et al. Clinical events in association with timing of intraventricular hemorrhage in preterm infants. J Pediatr 1992;121(4):614–9.
[34] Arduini D, Rizzo G, Romanini C, Mancuso S. Hemodynamic changes in growth retarded fetuses during maternal oxygen administration as predictors of fetal outcome. J Ultrasound Med 1989;8(4):193–6.
[35] Edelstone DI, Peticca BB, Goldblum LJ. Effects of maternal oxygen administration on fetal oxygenation during reductions in umbilical blood flow in fetal lambs. Am J Obstet Gynecol 1985;152(3):351–8.
[36] Nicolaides KH, Campbell S, Bradley RJ, Bilardo CM, Soothill PW, Gibb D. Maternal oxygen therapy for intrauterine growth retardation. Lancet 1987;1(8539):942–5.
[37] Salihagić-Kadić A, Medić M, Jugović D, Kos M, Latin V, Kusan Jukić M, et al. Fetal cerebrovascular response to chronic hypoxia—implications for the prevention of brain damage. J Matern Fetal Neonatal Med 2006;19(7):387–96.
[38] Paulson OB, Strandgaard S, Edvinsson L. Cerebral autoregulation. Cerebrovasc Brain Metab Rev 1990;2(2):161–92.
[39] Mathew RJ. Postural syncope and autoregulation of cerebral blood flow. Biol Psychiatry 1996;40(9):923–6.
[40] Sundgreen C, Larsen FS, Herzog TM, Knudsen GM, Boesgaard S, Aldershvile J. Autoregulation of cerebral blood flow in patients resuscitated from cardiac arrest. Stroke 2001;32(1):128–32.
[41] Nishizawa H, Kudoh I. Cerebral autoregulation is impaired in patients resuscitated after cardiac arrest. Acta Anaesthesiol Scand 1996;40(9):1149–53.
[42] Immink RV, van den Born BJ, van Montfrans GA, Koopmans RP, Karemaker JM, van Lieshout JJ. Impaired cerebral autoregulation in patients with malignant hypertension. Circulation 2004;110(15):2241–5.
[43] Cruz J, Jaggi JL, Hoffstad OJ. Cerebral blood flow, vascular resistance, and oxygen metabolism in acute brain trauma: redefining the role of cerebral perfusion pressure? Crit Care Med 1995;23(8):1412–7.
[44] Agnoli A, Fieschi C, Bozzao L, Battistini N, Prencipe M. Autoregulation of cerebral blood flow. Studies during drug-induced hypertension in normal subjects and in patients with cerebral vascular diseases. Circulation 1968;38(4):800–12.
[45] Panerai RB. Assessment of cerebral pressure autoregulation in humans–a review of measurement methods. Physiol Meas 1998;19(3):305–38.
[46] Bickler PE. Cerebral anoxia tolerance in turtles: regulation of intracellular calcium and pH. Am J Physiol 1992;263(6 Pt 2): R1298–302.
[47] Bickler PE. Effects of temperature and anoxia on regional cerebral blood flow in turtles. Am J Physiol 1992;262(3 Pt 2): R538–41.
[48] Mortberg E, Cumming P, Wiklund L, Wall A, Rubertsson S. A PET study of regional cerebral blood flow after experimental cardiopulmonary resuscitation. Resuscitation 2007;75(1): 98–104.
[49] Laudignon N, Farri E, Beharry K, Rex J, Aranda JV. Influence of adenosine on cerebral blood flow during hypoxic hypoxia in the newborn piglet. J Appl Physiol 1990;68(4): 1534–41.
[50] Strouse JJ, Cox CS, Melhem ER, Lu H, Kraut MA, Razumovsky A, et al. Inverse correlation between cerebral blood flow measured by continuous arterial spin-labeling (CASL) MRI and neurocognitive function in children with sickle cell anemia (SCA). Blood 2006;108(1):379–81.
[51] Prohovnik I, Pavlakis SG, Piomelli S, Bello J, Mohr JP, Hilal S, et al. Cerebral hyperemia, stroke, and transfusion in sickle cell disease. Neurology 1989;39(3):344–8.
[52] Chi OZ, Hunter C, Liu X, Chi Y, Weiss HR. Effects of GABA(A) receptor blockade on regional cerebral blood flow and blood-brain barrier disruption in focal cerebral ischemia. J Neurol Sci 2011;301(1–2):66–70.
[53] Mountz JM. Nuclear medicine in the rehabilitative treatment evaluation in stroke recovery. Role of diaschisis resolution and cerebral reorganization. Eura Medicophys 2007;43(2): 221–39.
[54] Moguel-Ancheita S, Orozco-Gómez LP, Gallego-Duarte M, Alvarado I, Montes C. Metabolic changes in brain cortex related with the strabismus treatment. Preliminary results with SPECT. Cir Cir 2004;72(3):165–70.
[55] Biagi L, Abbruzzese A, Bianchi MC, Alsop DC, Del Guerra A, Tosetti M. Age dependence of cerebral perfusion assessed by magnetic resonance continuous arterial spin labeling. J Magn Reson Imaging 2007;25(4):696–702.